K = equilibrium constant
L = liquid flow rate
N = number of theoretical plates
N_{SS} = number of actual plates in SS condition
P = pressure
T = temperature
t = time
t_v = vapor flow time
u = input
V = vapor flow rate
X = dimensionless liquid composition
x = liquid composition
x' = liquid composition difference
y = vapor composition
ϵ = plate efficiency
θ = dimensionless time
λ = mV/L
η = fraction of liquid holdup transferred per cycle

LITERATURE CITED

AIChE Research Committee, "Tray Efficiencies in Distillation Columns," Final Report., Univ. Delaware, Newark (1958).

Biddulph, M. W., and D. J. Stevens, "Oscillating Behaviour on Distillation Trays," *AIChE J.*, **20**, No. 1, 60 (1974).

Chien, H. H., J. T. Sommerfeld, V. N. Schrodt, and P. E. Parisot, "Study of Controlled Cyclic Distillation: 11," *Sep. Sci.*, 1, Nos. 2 and 3, 281 (1966).

Dale, E. B., "Variable Time Control of a Periodically Cycled Plate Column," Ph.D. thesis, Univ. Sydney, Australia (1976).

Duffy, G. J., "Periodic Cycling of a Large Diameter Plate Column," Ph.D. thesis, Univ. Sydney, Australia (1976).

Furzer, I. A., and G. J. Duffy, "Generalized Theory of Periodically Operated Plate Columns," Joint Symposium on Distillation, Univ. Sydney/Univ. of NSW, Australia (May, 1974).

———, "Periodic Cycling of Plate Columns: Discrete Residence Time Distribution," *AIChE J.*, **22**, No. 6, 1118 (1976).

Gerster, J. A., and H. M. Scull, "Performance of Tray Columns Operated in the Cycling Mode," *ibid.*, **16**, No. 1, 108 (1970).

Hinze, J. O., "Oscillations of a Gas/Liquid Mixture on a Sieve Plate," Proc. Symp. on Two Phase Flow, Exeter. Dept. of Chem. Eng., Univ. of Exeter, 2, F102 (1965).

McAllister, R. A., Ph.H. McGinnis, Jr., and C. A. Plank, "Perforated Plate Performance," *Chem. Eng. Sci.*, 9, 25 (1958).

McCann, D. J., and R. G. H. Prince, "Bubble Formation and Weeping at a Submerged Orifice," *Chem. Eng. Sci.*, **24**, 801 (1969).

McWhirter, J. R., and W. A. Lloyd, "Controlled Cycling in Distillation and Extraction," *Chem. Eng. Progr.*, **59**, No. 6, 58 (1963).

Schrodt, V. N., J. T. Sommerfeld, O. R. Martin, P. E. Parisot, and H. H. Chien, "Plant-Scale Study of Controlled Cyclic Distillation," *Chem. Eng. Sci.*, **22**, 759 (1967).

Zanelli, S., and R. Del Bianco, "Perforated Plate Weeping," *Chem. Eng. J.*, **6**, 181 (1973).

Manuscript received June 6, 1977; revision received December 23, and accepted January 5, 1978.

A Design Oriented Model of Fines Dissolving

Mass and population balances, together with nucleation kinetics of the potassium chloride system, were combined to present a design oriented model which describes the behavior of a fines destruction system (FDS) implemented in an MSMPR crystallizer. This model was tested in a well-documented, bench scale, potassium chloride crystallizer and was found to be adequate to predict the effect of fines dissolving. Product size improvement was related to incremental cost incurred with an FDS.

ZLATICA I. KRALJEVICH

and

ALAN D. RANDOLPH

Department of Chemical Engineering
The University of Arizona
Tucson, Arizona 85721

SCOPE

An industrially used technique for making a larger sized crystal product from a mixed magma crystallizer is to segregate fine crystals from the magma, dissolve them, and recycle the dissolved solute for further growth on existing crystals. This technique permits the same production to be made on fewer numbers of crystals of larger average size. The growth rate is forced to a higher level to produce the same mass on a smaller crystal surface area. As with most process advances, the industrial practice of fines dissolving predates the rigorous design and analysis of such techniques.

The present work presents an experimental study of a mixed magma potassium chloride crystallizer equipped with a fines segregation and destruction system. The objectives of the study were to demonstrate in a well-documented, bench scale apparatus the utility and applicability of the R parameter fines dissolving model as well as to present a design oriented technique for solution of the model equations for rapid design and analysis calculations of fines removal systems. A final objective was to relate the relative size improvement of crystal product with incremental costs incurred with a fines dissolving system.

CONCLUSIONS AND SIGNIFICANCE

The general validity of the R parameter fines dissolving model was supported by this experimental study. Certainly, the relative slopes of the fines and product segments from semilog population plots were in close agreement with the respective removal rates in the two size ranges. However, the point of intersection of these two straight line segments, which represents the maximum fines size L_F in the idealized dissolving model, was always less than both the value of L_F calculated from settling rate correlations and maximum sizes presumably observed in the fines stream with the particle counter. However, this discrepancy does not prevent reasonable a priori engineering design calculations of expected size improvement using only Stokes law types of correlations to design a fines settler. The size improvement prediction would become quite good if the empirical discrepancy presented in this paper between L_F values (settling rate vs. break point on semilog plot) is found to be valid for other systems.

A problem which previously limited use of the fines dissolving model has been graphically solved in the present study, namely, the trial and error simultaneous solution of the population balance/mass balance/nucleation kinetics relationships which required computer implementation. The graphical short-cut techniques presented in this paper should greatly enhance the utility of this model as a rapid and useful analysis tool which would be sufficiently accurate for most engineering applications. All that is needed to make a quick estimate of size improvement is a value for the characteristic size ($G\tau$) under MSMPR (mixed suspension mixed product removal) conditions with the same retention time, the relative nucleation/growth rate sensitivity parameter i, and the system dissolving parameters to be studied, for example, L_F, Q_R.

The fraction of fines dissolved and recycled (relative to net production rate) can easily be calculated using the graphical technique presented here. These calculations revealed that there is an upper limit (for each dissolving ratio R) on the dissolving parameter λ after which the fraction of fines dissolved is constant, although calculated particle size (as $G\tau$) continues to increase. In a practical sense, this limit is achieved when essentially all originally formed nuclei have been exponentially decimated (reduced by the factor $e^{-\lambda}$) within the size range $(0, L_F)$. Thus, product mass occurs mainly in the fines size range and the fines dissolving and production rates are in the same ratio as their respective flows, that is, $R - 1$. This total washout of fines with excessive dissolving has been reported in industrial systems and could easily account for the wild CSD oscillations observed in these industrial crystallizers.

Saeman, in 1956, first published a study of CSD which included a fundamental analysis of the mass-number-size relationships inherent in the MSMPR crystal distribution. This study clearly set forth the requirements for, and probable consequences of, a fines dissolving system associated with a mixed magma crystallizer. However, a detailed CSD model for fines destruction awaited the formalization of CSD studies (in a reactor engineering sense) utilizing the population balance concept. Larson and Randolph (1969) first parameterized a CSD model for fines dissolving in which the total fines removal rate (product plus dissolver) was R times the product removal rate. As the mean retention time is inversely proportional to the removal rate, the principal effect of fines removal is to achieve a size dependent separation of residence time probabilities between fines and product sized crystals. Thus, in terms of the above idealized model

$$\tau_{\text{fines}} = \frac{\tau_{\text{product}}}{R}$$

The R parameterized fines dissolving model was formalized with associated mass balance and kinetics expressions (Randolph and Larson, 1971) to give a complete engineering description of a mixed magma crystallizer with fines removal. Although such CSD models are being utilized in practical engineering studies, little published work has appeared to document their veracity and reliability. Recently, Juzaszek and Larson (1977), have observed the characteristic CSD forms predicted by the idealized R parameter model, thus supporting the principal assumption of size dependent residence times. The present study utilizes the original R parameterized model, simplifying the mass balance constraint to present the model in a more design useful form.

THE MODEL

The population balance, extensively discussed by Randolph and Larson (1971), is the starting point for a CSD model of a crystallizer with fines dissolver. Thus, if we consider a size dependent removal rate $Q(L)$, the mean residence time probability at a size L becomes

$$\tau(L) = \frac{V}{Q(L)} = \begin{cases} \tau_p/R & L < L_F \\ \tau_p & L > L_F \end{cases} \tag{1}$$

and where $\tau_p = V/Q_p$ is the mean retention time of product sized crystals.

For the steady state MSMPR crystallizer with fines dissolver, the population balance becomes simply

$$\frac{dn}{dL} = -\frac{n}{G\tau(L)} \tag{2}$$

with the steady state solution

$$n = n^o \exp\left[-\int_0^L \frac{dL}{G\tau}\right] \tag{3}$$

Equation (3) plots as a straight line on semilogarithmic graph paper, where n^o represents the intercept of this line at zero size, as shown in Figure 1. The slope of the line is equal to $-1/G\tau$. When the crystallizer is equipped with a fines trap and fines destruction system (FDS), two different CSD straight line segments are obtained as shown in Figure 1. The slope of the fines CSD has the value of $-R/G\tau$, where $R = 1 + Q_R/Q_P$, Q_R being the fines removal rate. Continuity of the distribution at L_F, the largest size of particles being destroyed, is assumed. Thus, given the form of the CSD

with an FDS [Equation (3)], experimental values for nuclei density n^o, growth rate G, and maximum dissolving size L_F can be obtained from the intercept, slope, and line segment intersection, respectively, on a population density plot, as shown in Figure 1.

The usefulness of a fines destruction system in improving the average size of crystallized product is largely recognized. The exact behavior of the fines trap can be obtained by solving the appropriate mass and population balances, together with the nucleation kinetics of the system.

A simplified model has been presented by Randolph and Larson (1971), which gives the size improvement with fines destruction as

$$\frac{L_{d2}}{L_{d1}} = \left[\frac{1}{\beta}\right]^{1/i+3} = e^{\lambda/i+3} \tag{4}$$

L_d is the dominant crystal size (weight basis) given as $L_d = 3G\tau$ for the MSMPR distribution.

The parameter λ is the exponential decay ratio given by

$$\lambda = \frac{L_F(R-1)}{G_2\tau} = -\ln\beta \tag{5}$$

and the parameter i is a measure of the nucleation growth rate sensitivity.

In the development of Equation (4), it was assumed that the mass of the fines destroyed is negligible compared to the product, that is, a point fines trap. For this case, fines dissolving does not significantly perturb the form of the exponential distribution, and the effect of the fines distribution on the weight averaged size is neglected; that is, the product distribution is extrapolated to size zero to calculate L_d.

In a class II crystallizer (low supersaturation, high yield) with a point fines trap, both solids concentration and retention time remain invariant when fines destruction is implemented. Thus

$$M_{T2} = M_{T1} \tag{6}$$

or

$$\rho k_v \int_0^\infty n_1 L^3 dL \cong \rho k_v \int_0^\infty n_2 L^3 dL \tag{7}$$

The slurry density M_T for the case of an exponential distribution is given as

$$M_T = 6\,\rho k_v n^o (G\tau)^4 \tag{8}$$

This relationship is approximately true for the point FDS.

A more rigorous expression for size improvement for the case where the mass of fines destroyed is not negligible can be obtained by writing Equation (7) over both segments of the FDS distribution. Thus

$$\int_0^\infty n_1 L^3 dL = \int_0^{L_F} n_2 L^3 dL + \int_{L_F}^\infty n_2 L^3 dL \tag{9}$$

where n_1 and n_2 are the population density without and with fines dissolving.

In the case of an exponential distribution

$$\begin{aligned} n_1 &= n^o{}_1 \exp(-L/G_1\tau) && 0 < L < \infty \\ n_2 &= n^o{}_2 \exp(-LR/G_2\tau) && 0 < L < L_F \\ n_2 &= \beta n^o{}_2 \exp(-L/G_2\tau) && L_F < L < \infty \end{aligned} \tag{10}$$

Bringing (10) to (9) and using Equation (8), we get

$$n^o{}_1(G_1\tau)^4 \int_0^\infty e^{-x} x^3 dx = n^o{}_2(G_2\tau)^4 \int_0^{x_f} e^{-Rx} x^3 dx + \beta n^o{}_2(G_2\tau)^4 \int_{x_F}^\infty e^{-x} x^3 dx \tag{11}$$

where $x = L/G\tau$.

Making use of the incomplete gamma function given as

$$\omega(t) = \frac{1}{6}\int_0^t e^{-p} p^3 dp \tag{12}$$

we can rewrite Equation (11):

$$n^o{}_1(G_1\tau)^4 = \frac{n_2{}^o(G_2\tau)^4}{R^4}\omega(Rx_F) + \beta n_2{}^o(G_2\tau)^4[1-\omega(x_F)] \tag{13}$$

Or, rearranging, we get

$$1 = \left[\frac{G_2\tau}{G_1\tau}\right]^4 \frac{n^o{}_2}{n^o{}_1}\left\{\frac{\omega(Rx_F)}{R^4} + \beta[1-(x_F)]\right\} \tag{14}$$

If we assume nucleation growth rate kinetics of the form $n^o = k_N G^{i-1} M_T{}^j$ for a constant slurry density and retention time, this expression can be written as

$$\frac{n^o{}_2}{n^o{}_1} = \left[\frac{G_2}{G_1}\right]^{i-1} = \left[\frac{G_2\tau}{G_1\tau}\right]^{i-1} = \left[\frac{L_{d2}}{L_{d1}}\right]^{i-1} \tag{15}$$

Combining (14) with (15), we obtain an expression for size improvement:

$$\left[\frac{L_{d2}}{L_{d1}}\right]^{i+3} = \frac{1}{\dfrac{\omega(Rx_F)}{R^4} + \beta[1-\omega(x_F)]} \tag{16}$$

If we substitute $\beta = e^{-\lambda}$ and $x_F = LF/G\tau = \lambda/(R-1)$, the more general expression for size improvement is obtained:

$$\frac{G_2}{G_1} = \frac{L_{d2}}{L_{d1}}$$

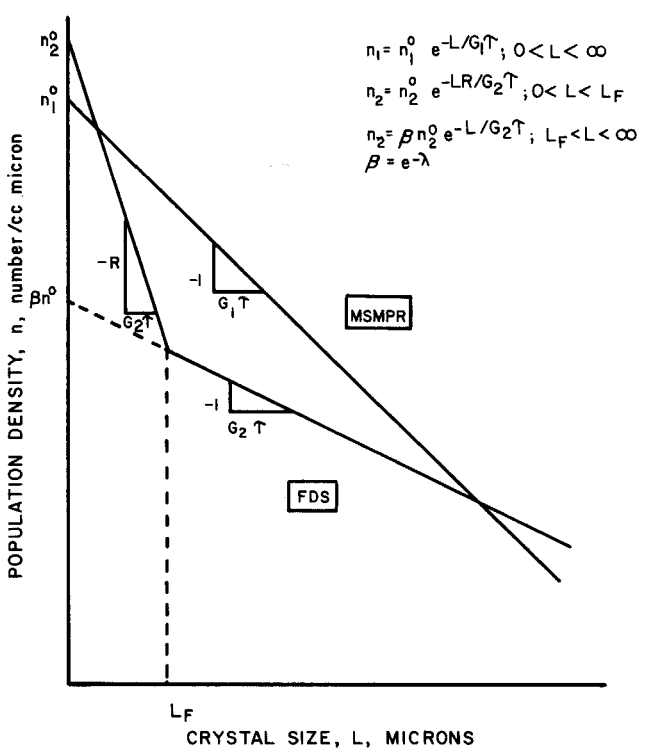

Fig. 1. Steady state comparison of MSMPR and FDS crystal size distribution.

$$= \left\{ \frac{1}{\frac{\omega(\lambda R/R-1)}{R^4} + e^{-\lambda}[1-\omega(\lambda/R-1)]} \right\}^{1/i+3} \tag{17}$$

Since $L_d = 3G\tau$, then $L_{d_2}/L_{d_1} \doteq \exp(\lambda/i+3)$ for the point FDS. Equation (4) allows the mass balance constraint to be expressed simply as

$$G_2 = G_1 \exp\left[\frac{\lambda}{i+3}\right] \tag{18}$$

Or, from the definition of the dissolving parameter [Equation (5)], the decay ratio must satisfy the equation

$$\lambda \exp(\lambda/i+3) = \frac{L_F Q_R}{G_1 V} = K \tag{19}$$

Equation (19) is essentially a mass balance constraint for a class II system with a point FDS. In order to solve Equation (19) for a specific design situation, a value for L_F must be estimated from a Stokes law type of correlation or obtained from experimental data (for example, pilot plant crystallizer with fines destruction). Simple MSMPR experiments provide the value of G_1 and a good estimate of the parameter i. When the value of λ is found from Equation (19), the size improvement ratio L_{d_2}/L_{d_1} can be calculated directly.

The total net production rate is given as

$$P = Q_p \rho k_v \int_0^\infty nL^3 dL$$

$$= Q_p \rho k_v \left[\int_0^{L_F} nL^3 dL + \int_{L_F}^\infty nL^3 dL \right] \tag{20}$$

Similarly, the rate of fines destroyed is

$$P_F = Q_R \rho k_v \int_0^{L_F} nL^3 dL \tag{21}$$

Thus, the fraction which is destroyed relative to net production ϕ can be expressed as

$$\phi = \frac{P_F}{P} = \frac{Q_R \int_0^{L_F} nL^3 dL}{Q_P \left[\int_0^{L_F} nL^3 dL + \int_{L_F}^\infty nL^3 dL \right]} \tag{22}$$

For an exponential distribution of the form of Equation (3), the fraction dissolved becomes

$$\phi = \frac{Q_R n^o (G\tau)^4 \int_0^{x_F} e^{-Rx} x^3 dx}{Q_p n^o (G\tau)^4 \left[\int_0^{X_F} e^{-Rx} x^3 dx + \int_{x_F}^\infty e^{-x_F(R-1)} e^{-x} x^3 dx \right]} \tag{23}$$

where $e^{-x_F(R-1)} = e^{-\lambda} = \beta$. Since $Q_R = (R-1)Q_P$, and letting $Rx = p$, this equation becomes

$$\phi = \frac{\frac{R-1}{R^4} \int_0^{Rx_F} e^{-p} p^3 dp}{\frac{1}{R^4} \int_0^{Rx_F} e^{-p} p^3 dp + e^{-x_F(R-1)} \int_{x_F}^\infty e^{-x} x^3 dx} \tag{24}$$

Using the definition given by Equation (12) for the gamma distribution, we get

$$\phi = \frac{\frac{R-1}{R^4} \omega(Rx_F)}{\frac{1}{R^4} \omega(Rx_F) + e^{-x_F(R-1)}[1-\omega(x_F)]} \tag{25}$$

The dissolving function can be expressed uniquely as a function of the dissolving parameter λ and dissolving ratio R. Thus

$$\phi = \frac{R-1}{1 + R^4 e^{-\lambda}\left[\frac{1-\omega(\lambda/R-1)}{\omega(R\lambda/R-1)}\right]} \tag{26}$$

It should be noted in the above development that the expression for ϕ is rigorous for all dissolving conditions if the parameter λ is known exactly, while the size improvement ratio calculation is based on a point FDS. If the rigorous expression for size improvement ratio [Equation (17)] is used, the dissolving parameter λ should itself be found by a trial and error solution of Equation (9) to obtain the FDS growth rate G_2. In any case, the approximate (point FDS) value for λ can be used in the rigorous expression for ϕ, but with some slight error.

EXPERIMENTAL

The crystallization equipment and general procedure used in this study have been previously described by Randolph et al. (1977). The crystallizer was equipped with a fines trap and a fines destruction system. Neither product classification nor clear liquor advance were implemented. The laboratory fines destruction system consisted of a steam heater unit, a holding tank, and a cooler unit. A temperature rise through the heater of about 10°C was required to totally dissolve the fines with a heater residence time of about 1 min.

A mean residence time of 45 min was obtained in the crystallizer. Three different levels of the fines removal rate Q_R were investigated. In addition, the crystallizer was run in the MSMPR mode with no fines destruction loop.

The size distribution of the product was obtained from sieve analysis. The distribution of the crystals in the fines loop was determined using a Coulter counter model T electronic particle analyzer. The nuclei captured by the trap had a maximum size of approximately 150 μ.

The nucleation growth rate kinetics of the potassium chloride system were previously obtained (Randolph et al., 1977) from both steady state and dynamics runs. These data were correlated using a conventional power law model as

$$B^\circ = 0.657\, G^{4.99} M_T^{0.14}$$

Steady state data from this study which were utilized in this correlation are summarized in Table 1.

The effect of trap velocity (given by the ratio between the volumetric fines rate and the cross-sectional area of the trap) on fines size L_F was studied at different fines rates Q_R and with a different fines trap area, thus independently changing trap velocity.

Further, an experimental determination of the settling velocity for potassium chloride crystals was performed. These measurements were done using a 1 000 cm^3 graduated cylinder filled with saturated potassium chloride solution and immersed in a thermostatic bath whose temperature was 40°C, the same as the crystallizer temperature. Potassium chloride crystals at different known sizes were dropped into the solution, and the time required for the particles to fall a predetermined distance was measured with a timer.

DISCUSSION OF RESULTS

The population density plots shown in Figures 2 and 3 were prepared as follows. The cumulative weight fraction distribution $\left[W = \rho k_v \int_0^{L} p^3 n(p)\, dp/M_T \right]$ was calculated from a sieve analysis of the crystallizer product

Table 1. Summary of Steady State MSMPR and FDS Experimental Results

Exp	Q_R (cm³/min)	Mode	n^o (#/cm³-μm)	G (μm/min)	M_T (g/l)	L_F (μm)
62 176	0	MSMPR	32	2.2	40	—
70 676	0	MSMPR	24	2.4	45	—
70 176	1 520	FDS	71	3.0	42	55
72 876	1 515	FDS	42	3.1	64	30
80 476	1 550	FDS	58	3.2	64	52
31 677	1 500	FDS	456	2.5	55	90
111 176	2 200	FDS	500	3.1	50	82
60 776	2 920	FDS	1 160	4.7	44	135
20 377	3 000	FDS	1 000	4.1	63	130
71 576	2 990	FDS	600	4.6	43	150
70 676	3 540	FDS	600	5.0	43	130

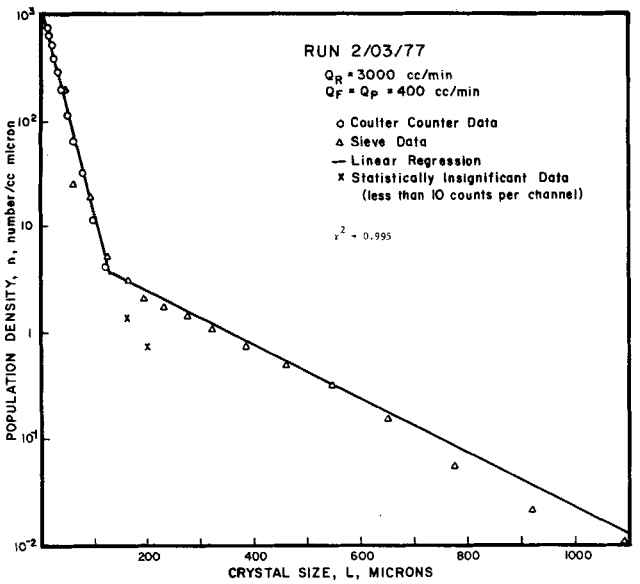

Fig. 2. Representative CSD produced with FDS in operation, good fit.

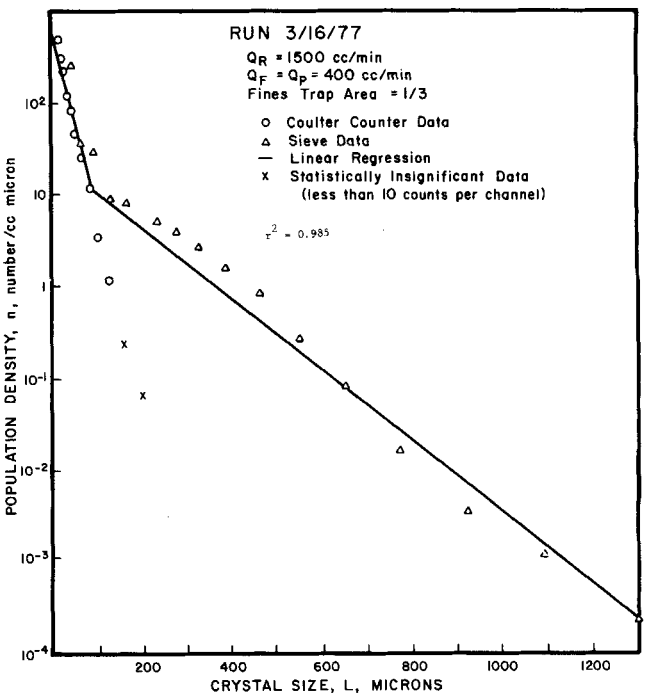

Fig. 3. Representative CSD produced with FDS in operation, poor fit.

and plotted vs. the crystal size L. Next, the weight distribution function ω was graphically determined from derivatives of the $W(L)$ plot. Values of the population density were then calculated as $n = \omega M_T/\rho k_v \overline{L}^3$, where $\overline{L}$ is the average size between two consecutive sieve screens. The best straight line was fit to these points by linear regression. The correlation line corresponds to the solid lines in Figures 2 and 3 with respective correlation coefficients of $r^2 = 0.995$ and 0.985. The two plots are representative of good and poor data fits to Equation (3). Actual population density values as calculated directly from the sieve analysis [no smoothing of the $W(L)$ curve] are shown in these figures, represented by the symbol Δ. Thus, the data smoothing technique described above was in reasonable agreement with raw population density values.

The largest particle size being dissolved in the fines loop L_F is one of the parameters that has to be considered in the design of a fines destruction system. L_F was determined from population density plots as previously described. L_F values depend upon the settling velocity which exists inside the fines trap. If the dependency of L_F on the velocity v for a given system can be calculated from a settling correlation, then L_F can be predicted and used in the proper design equations. However, if this relationship is unknown, the fines size would have to be obtained experimentally in a pilot plant crystallizer with fines loop or estimated in order to design the FDS.

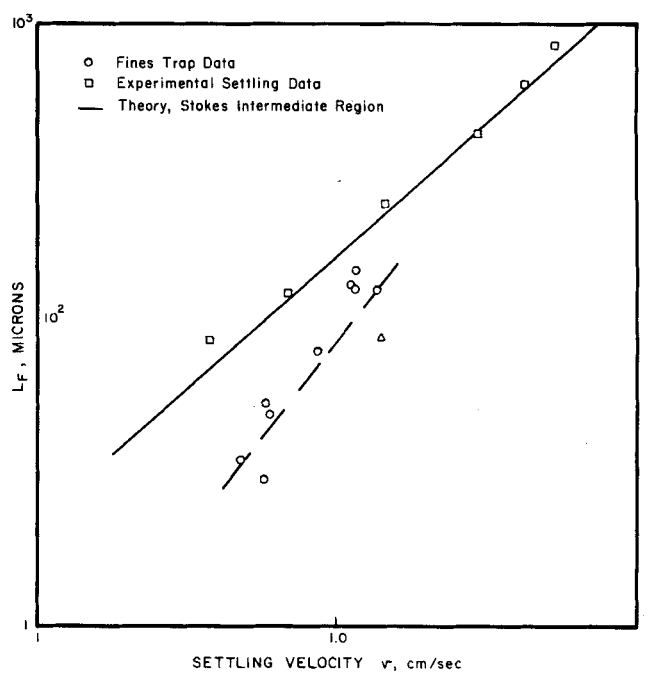

Fig. 4. Theoretical and experimental correlations between the critical size L_F and the settling velocity inside the fines trap.

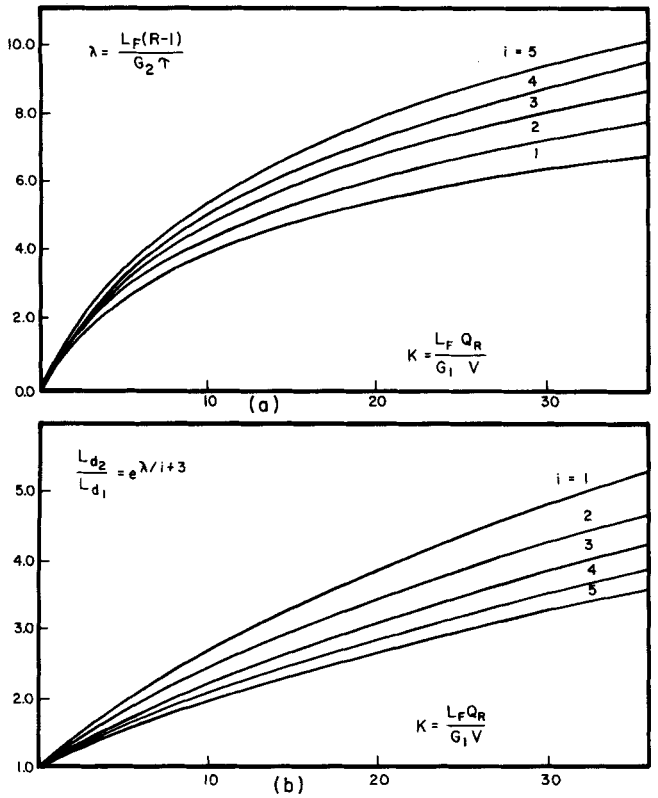

Fig. 5. Design correlations for size improvement with FDS.

For the potassium chloride system, the theoretical dependence of L_F on v (expressed by a Stokes type of correlation corresponding to values of Re between 0.5 and 2) is given as

$$L_F = 168\, v^{0.875} \tag{27}$$

Multiple linear regression of experimental L_F values (from semilog population plots) data gave the correlation

$$L_F = 96\, v^{1.276} \tag{28}$$

The theoretical (Stokes type) and experimental (semilog intersection) correlations for L_F are shown in Figure 4. In this figure, the datum point indicated by Δ corresponds to an experiment carried out with a fines trap area equal to one third of the total trap area. Figure 4 plots data points from the experimental determination of potassium chloride settling velocity.

Although L_F values obtained from the CSD analysis were found to increase with fines trap velocity, they were still lower than the values predicted from settling theory. This might be explained by the small ratio of removal tube to trap cross-sectional area. Thus, internal circulation patterns within the trap may have been set up which prevented the larger particles from reaching the outlet tube. With the small outlet/trap area ratio, a stagnant zone would surely exist in the upper section of the trap away from the outlet. Of course, if this conjecture is to explain the low L_F values, a circulating flow at some point within the trap must be postulated that would ultimately allow the larger particles to exit back to the magma.

It was observed that values of L greater than L_F were apparently measured by the Coulter counter in the fines loop stream (see Figures 2 and 3). This result has been reported in the literature, although not completely explained. Helt and Larson (1976) attribute this result to the existence of a parabolic velocity profile inside the fines trap due to laminar flow which entrains some crystals larger than expected, based on the average flow rate. A fluid velocity higher than the mean velocity would then exist at the center of the trap carrying crystals of larger size. However, if particles at sizes greater than L_F were actually being removed from the trap at the fines rate, a noticeable effect on the product CSD should be observed; that is, the line representing the product distribution would be shifted downwards. Sieve analysis did not show such an effect, indicating that fines larger than L_F were not effectively being removed, at least as far as the effect on CSD was concerned.

This suggests that these data points are apparent, perhaps owing to coincidence or noise when using the Coulter counter. Data points that are close to the real distribution, that is, at sizes not much greater than L_F, might have been caused by coincidence; that is, two particles of a small size are counted at the same time by the counter. Thus, the equipment detects a doubled volume and associates it to a size which is larger than the real size. This explanation of spurious counts is borne out by the fact that similar size channels were populated regardless of the value of L_F.

The equations necessary to design a fines destruction system have been previously derived for the specific case of a point fines trap, that is, negligible fines mass dissolved, and for the more general case of dissolving larger particles, as given by Figure 5*b* and Equation (17). respectively. The fines-to-product mass ratio which limits the proper use of the point fines trap approximation has never been specifically investigated. However, it is generally accepted that this ratio should be less than 5% for the point fines trap assumption to hold. Larson and Garside (1973) assume the point fines trap approximation is valid if the destroyed fines are less than 10 μm. Calculations of the size improvement for experiments carried out during this study have shown that the simpler approximation [Equation (4) and Figure 5*b*] holds for fines-to-product ratios as high as 35% with only 2% error.

In order to estimate the size improvement with fines destruction either from Equation (4) or Equation (17), the value of the exponential decay ratio λ must be determined from the mass balance constraint, Equation (9) (rigorous) or Equation (19) (approximate). In order to solve Equation (19), the ratio K and the parameter i must be known. If the relative kinetic order of nucleation to growth i is unknown, it can be estimated with a good approximation from two MSMPR runs. The same MSMPR experiments will provide the value of the growth rate G_1. The fines removal rate Q_R is set by choice, while L_F can be estimated from settling correlations or experimentally obtained. Equation (19) was solved numerically using Newton's method, and the results are shown in Figure 5*a* for different values of the kinetic parameter i.

With i and λ known, the size improvement with fines destruction can be directly obtained from Equation (4). In order to make use of Equation (17), the incomplete third-order gamma function must be obtained for the corresponding values of λ and $R = 1 + Q_R/Q_P$.

Size improvement calculated from Equation (4) has been plotted vs. K as shown in Figure 5*b*. If the design engineer is interested in determining size improvement only, then the intermediate step of determining λ is not necessary, and Figure 5*b* can be used directly.

The fraction of net production which is dissolved and recycled can be calculated from Equation (26). The dissolved fraction ϕ is plotted vs. λ in Figure 6 for different values of R. This figure has considerable interest from the design viewpoint because it shows that for a given value of R there exists a limiting value of λ over which the dissolved fraction no longer increases. This asymp-

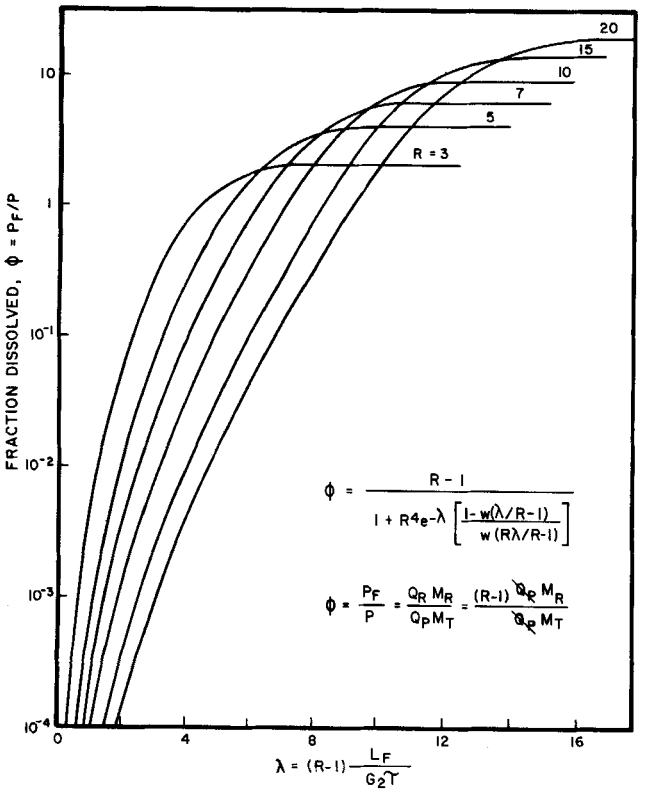

Fig. 6. Fraction of fines dissolved vs. exponential decay ratio, λ.

totic value for each curve corresponds to $(R - 1)$. Some insight into this physical limit can be obtained as follows. The fraction dissolved and recycled can be expressed as

$$\phi = \frac{P_F}{P} = \frac{Q_R M_R}{Q_P M_T} \tag{29}$$

As $Q_R = (R - 1)Q_P$, Equation (29) becomes

$$\phi = \frac{(R-1)M_R}{M_T} \tag{30}$$

Thus, when $\phi = R - 1$, the distribution of the fines corresponds to the entire distribution, and the product is obtained in the same ratio to the fines dissolved as their respective flows. Note that dominant size as expressed by the variable $3G_T$ is still predicted to increase. However, this would not in fact be true. As the product distribution approached the fines distribution, the approximation $L_d \doteq 3G_T$ would be very poor indeed, as the entire fines distribution is omitted from this approximation. If a rigorous statistical definition for L_d were employed, then product size would indeed decline at some level of dissolving given by high values of the parameter λ.

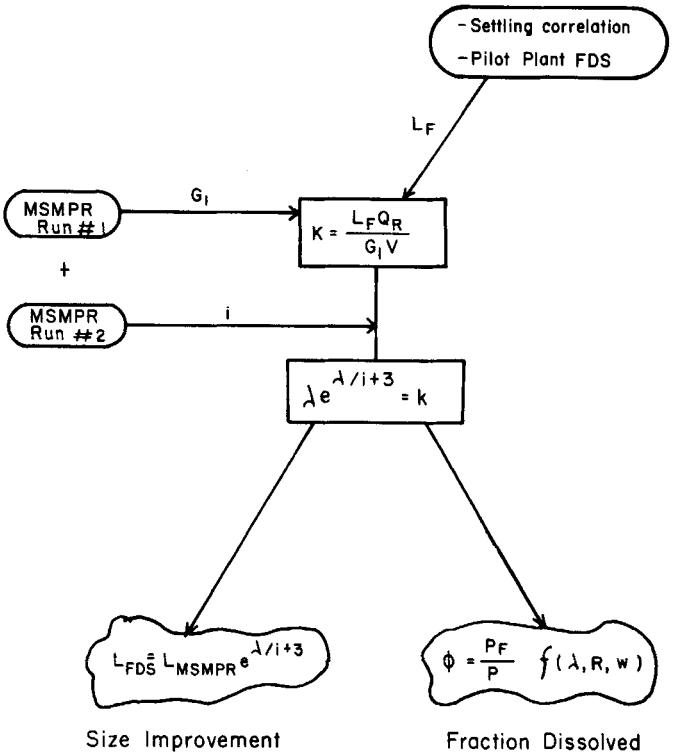

Fig. 7. Decision flow diagram for size improvement analysis.

There exists, then, a physical limitation for the values of λ. For any realistic design, the fines trap operating conditions must be such that the critical value of λ will not be reached. Different combinations of R and L_F result in equivalent values of the parameter λ. Which values are chosen is an economic decision. Large values of R mean larger flow rates which makes the operation more expensive. On the other hand, large values of L_F are impractical because of the difficulty in dissolving such large particles. Figure 7 shows a decision flow diagram for such a size improvement analysis. To utilize the procedures of Figure 7, the following information and/or actions are required:

1. A simple MSMPR run provides the value of G_1.
2. L_F is estimated from a settling correlation or experimentally obtained by the method of semilog plot intersections from pilot scale operation.
3. Q_R is set by choice.
4. The volume of the reactor V is known.
5. K is calculated from $K = L_F Q_R / G_1 V$.
6. An additional MSMPR run allows estimation of the nucleation parameter i.
7. With i known, λ can be graphically obtained (Figure 5*a*) for any value of K.
8. With i known, the size improvement ratio can be graphically determined (Figure 5*b*) for any value of K.

TABLE 2. EXPERIMENTAL AND PREDICTED SIZE IMPROVEMENT

$G_1 = 2.3\ \mu m/min$ $\quad i = 5$
$V = 18\,000\ cm^3$ $\quad K = L_F Q_R / G_1 V$

R	Q_R (cm³/min)	L_F, exp. (μm)	K	λ	ϕ (%)	Size improvement, L_{d2}/L_{d1} Equation (4) approximate (a)	(b)	(c)	Equation (17), exact (a)	Experimental size improvement
4.8	1 500	55	2.0	2.0	1.3	1.28	1.40	1.20	1.30	1.30
6.5	2 200	82	4.4	3.3	4.5	1.51	1.75	1.42	1.53	1.35
8.5	3 000	150	11.0	5.7	35.0	2.04	2.20	1.80	2.03	2.00

(a). Using the experimental semilog intersection for L_F.
(b). Using the theoretical settling correlation for L_F, Equation (27).
(c). Using the experimental settling correlation for L_F, Equation (28).

Table 3. Fines Destruction by Dilution vs. Heating Technique

R	Dilution total cost ($/ton of product)	Heating total cost ($/ton of product)	Expected size improvement (L_{d2}/L_{d1})
3	0.109	4.99	1.08
5	0.224	9.97	1.25
7	0.329	14.97	1.50
10	0.532	22.50	2.16
15	2.050	35.03	3.40

9. Finally, for a given value of R, the fraction dissolved and recycled can be graphically determined (Figure 6) for any value of λ.

Data collected for three FDS experiments in this study were used to determine the size improvement by using Equations (4) and (17), along with Figures 5*a*, 5*b*, and 6, using the system kinetics and operating parameters as experimentally determined. The results are summarized in Table 2. It can be observed that for a fraction of fines dissolved as high as 35%, Equation (4) is still an excellent approximation. However, it should be pointed out that the value of λ used in Equation (17) was obtained from the approximate mass constraint Equation (19). The experimental values of size improvement are given by the ratio between the growth rate at FDS conditions G_2 and the growth rate at MSMPR conditions G_1 for the same residence time. The values of G_2 were obtained from Table 1. G_1 was considered to be 2.3 μm/min from an MSMPR run with the same retention. The experimental and predicted values of size improvement are seen to be in excellent agreement. It is important to note that in this case the size improvement prediction is still acceptable, from an engineering standpoint, if the values of L_F are estimated from the theoretical Stokes type of correlation [Equation (27)]. Thus, the model should be generally applicable.

INCREMENTAL OPERATING COST WITH FDS

Fines dissolving can be accomplished using heating and/or dilution. On a laboratory scale, the fines particles can easily be destroyed by heating, as was done in the present study. Since heating requires a large amount of energy, fines would be destroyed by dilution rather than heating on an industrial scale, if at all possible.

Potassium chloride is produced industrially in a flash cooling crystallizer, where cooling is produced by flash evaporation. About 8 to 10% of the water content in the feed solution is flashed. Since the magma also contains sodium chloride, which is precipitated by evaporation, 50% of the flashed water is recycled to the crystallizer to maintain potassium chloride purity. If a fines destruction system is to be implemented on such a crystallizer, a logical and inexpensive procedure is to make use of the flashed water to dissolve the nuclei. This technique avoids increased operating costs for fines heating and provides the water necessary to maintain the required purity level. The fines stream coming out of the trap is mixed with dilution water in an auxilliary tank and then recycled to the crystallizer.

A rough estimation of the incremental operating cost for a crystallizer with a fines trap is shown in Table 3, as a function of the dissolving ratio R. Both dilution and heating techniques are compared for a given size improvement. Calculations were made based on the experimental conditions present in this study; however, the conclusions should apply to an industrial scale as well. The cost estimation for fines destruction considers pumps, piping, and power for pumping costs.

When dissolving the fines by dilution, it was found that the water flashed to produce the required cooling provides the necessary water to dissolve nuclei for a value of R up to 9. For values of R higher than 9, the difference between the available and the required water has to be supplied, and the additional water cost was considered in the calculations. No incremental steam costs to remove this extra water were considered.

The cited costs were obtained by standard engineering design and cost estimating techniques. They are perhaps not accurate in an absolute sense but certainly are valid to illustrate the relative cost differential between heating and dilution.

Obviously, for a desired size improvement, fines destruction by heating is expensive. Destruction of nuclei by dilution is perhaps the only feasible technique for large scale, low value industrial processes.

ACKNOWLEDGMENT

The authors are indebted to the National Science Foundation, Grant ENG75-04348, for support of this research.

NOTATION

G = growth rate
i = order of nucleation (supersaturation)
j = order of nucleation (suspension)
k_v = volumetric shape factor
L = particle size
L_d = dominant particle size
L_F = upper limit in fines destruction
M_R = slurry density in fines trap
M_T = slurry density in crystallizer
n = population density at size L
n^o = nuclei population density
P = production rate
P_F = fines production rate
Q = volumetric flow rate
Q_P = product volumetric flow rate
Q_R = fines volumetric flow rate
R = fines destruction rate $(Q_R + Q_P)/Q_P$
V = suspension volume
v = settling velocity
W = cumulative weight fraction distribution
x = dimensionless crystal size

Greek Letters

β = fraction of crystals surviving the fines trap
ϕ = fraction of net production
λ = exponential decay ratio
ρ = crystal density
τ = mean residence time
ω = weight distribution function

Subscripts

1 = without FDS
2 = with FDS

LITERATURE CITED

Helt, J. E., and M. A. Larson, "Effects of Temperature on the Crystallization of Potassium Nitrate by Direct Measurement of Supersaturation," paper presented at the World Congress on Chemical Engineering, Amsterdam, The Netherlands, (June 30, 1976).

Juzaszek, P., and M. A. Larson, "Influence of Fines Dissolving on Crystal Size Distribution in a MSMPR Crystallizer," *AIChE J.*, 23, 4, 460-468 (1977).

Larson, M. A., and J. Garside, "Crystallizer Design Techniques Using the Population Balance," *Chem. Eng.*, **161**, 318 (1973).

Larson, M. A., and A. D. Randolph, "Size Distribution Analysis

in Continuous Crystallization," *Chem. Eng. Prog. Symposium Ser. No. 65*, 1-11 (1969).
Randolph, A. D., J. R. Beckman, and Z. I. Kraljevich, "Crystal Size Distribution Dynamics in a Classified Crystallizer. Part I. Experimental and Theoretical Study of Cycling in a Potassium Chloride Crystallizer," *AIChE J.*, 23, No. 4, 500-510 (1977).
Randolph, A. D., and M. A. Larson, *Theory of Particulate Processes*, Academic Press, New York (1971).

Manuscript received July 19, 1977; revision received January 3, and accepted January 5, 1978.

A Rigorous Method for Calculating Minimum Reflux Rates in Distillation

A computer method has been developed to calculate the minimum reflux rate for a specified distillation separation. The method makes no unnecessary simplifying assumptions of the distillation process model. The limitation of the method is that it cannot solve problems in which the minimum reflux rate is determined by a point of tangent between the operating line and the equilibrium line on a McCabe-Thiele diagram (see Figure 1).

HENRY H. Y. CHIEN

Monsanto Company
800 N. Lindbergh Blvd.
St. Louis, Missouri 63141

SCOPE

The calculation of minimum reflux rates for specified distillation separations has long been one of the important problems in distillation calculations. The concept of minimum reflux is quite basic but useful in the design of distillation processes. Columns can be designed quickly and with confidence if the minimum reflux rate is known. Obviously, the designed reflux rate must always be greater than the minimum rate by a certain amount. This amount should be selected with considerations based on the certainty of the vapor-liquid equilibrium model as well as comparative costs of capital vs. utilities. If the equilibrium model in use is not accurate, or if costs of utilities are relatively low, one should choose a large ratio (1.3 or larger) of actual to minimum reflux. A known minimum reflux rate can therefore reduce significantly operating, start-up, and design costs of a distillation process.

Most of the well-known work published in the area of minimum reflux calculations appeared before the advent of high speed computers. Developed primarily for manual or low speed computer calculations, these methods used simplifying assumptions in order to save time. These assumptions often cause uncertain and inaccurate results. The more common of these assumptions are constant molal overflows (Underwood, 1948; McCabe and Thiele, 1925), constant relative volatilities (Underwood, 1948), binary distillation (Ponchon, 1921; Savarit, 1922; McCabe and Thiele, 1925), and known product compositions (Jenny, 1939).

Bachelor (1957) presented perhaps the best hand calculation method to date. His method did not contain any of the above assumptions; however, it used simplifying approximations in equilibrium and heat and material balances. Erbar and Maddox (1962) published a computer method using Bachelor's method with added refinements but did not include problems of superheated or subcooled feeds.

CONCLUSIONS AND SIGNIFICANCE

The method developed in this work is designed for use on a high speed computer and is rigorous in the sense that:

1. The vapor-liquid equilibrium relationship may be represented by any nonideal model.
2. Any component or mixture enthalpy model may be used.
3. All or any two components may be distributed between the distillate and the bottoms.
4. Plate material and energy balances are used where needed.
5. Overall column material and energy balances are satisfied at convergence.

The solution speed obviously depends on the complexity of physical property and equilibrium models used for the problem. But, in general, this method requires more computer time than is required by a rigorous distillation simulation program.

The most important and restrictive assumption used in the development of this method is that the pinch zone cannot be at a point where the operating line is tangent to the equilibrium surface (see Figure 1). Our experience indicated that the use of this method for such a problem resulted in large solution oscillations such that convergence was not possible. However, it has produced correct solutions to problems for which the minimum refluxes are negative.

0001-1541-78-1238-0606-$01.05.